Oncogene (2011) 30, 3792–3801

www.nature.com/onc

ORIGINAL ARTICLE

TXNIP potentiates Redd1-induced mTOR suppression through stabilization of Redd1

H-O Jin[1], S-K Seo[1], Y-S Kim[1], S-H Woo[1], K-H Lee[1], J-Y Yi[2], S-J Lee[3], T-B Choe[4], J-H Lee[4], S An[4], S-I Hong[1] and I-C Park[1]

[1]*Division of Radiation Cancer Research, Korea Institute of Radiological & Medical Sciences, Seoul, Republic of Korea;* [2]*Laboratory of Modulation of Radiobiological Responses, Korea Institute of Radiological and Medical Sciences, Seoul, Republic of Korea;* [3]*Laboratory of Molecular Biochemistry, Department of Chemistry, Hanyang University, Seoul, Republic of Korea and* [4]*Department of Microbiological Engineering, Kon-Kuk University, Seoul, Republic of Korea*

The mammalian target of rapamycin (mTOR) is a highly conserved serine–threonine kinase activated in response to growth factors and nutrients. Because of frequent dysregulation of the mTOR signaling pathway in diverse human cancers, this kinase is a key therapeutic target. Redd1 is a negative regulator of mTOR, mediating dissociation of 14-3-3 from tuberous sclerosis complex (TSC)2, which allows formation of a TSC–TSC2 complex. In the present study, we identify TXNIP that inhibits mTOR activity by binding to and stabilizing Redd1 protein. Redd1 and TXNIP expression was induced by a synthetic glucose analog, 2-deoxyglucose (2-DG). Moreover, Redd1 expression in response to 2-DG was regulated by activating transcription factor 4 (ATF4). Overexpression of TXNIP was associated with reduced mTOR activity mediated by an increase in Redd1 level, whereas knockdown of TXNIP using small interfering RNA resulted in recovery of mTOR activity via downregulation of Redd1 during treatment with 2-DG. Interestingly, Redd1 was additionally stabilized via interactions with N-terminal-truncated TXNIP, leading to suppression of mTOR activity. Our results collectively demonstrate that TXNIP stabilizes Redd1 protein induced by ATF4 in response to 2-DG, resulting in potentiation of mTOR suppression. To the best of our knowledge, this is the first study to identify TXNIP as a novel member of the mTOR upstream that acts as a negative regulator in response to stress signals.
Oncogene (2011) **30,** 3792–3801; doi:10.1038/onc.2011.102; published online 4 April 2011

Keywords: ATF4; mTOR; Redd1; TXNIP; 2-deoxyglucose

Introduction

The mammalian target of rapamycin (mTOR) is a highly conserved serine–threonine kinase that integrates signals from growth factors and nutrients to coordinate cell growth and proliferation by controlling cap-dependent translation (Schmelzle and Hall, 2000; Sudarsanam and Johnson, 2010). Dysregulation of mTOR signaling is implicated in various human diseases, including cancer, diabetes, obesity, neurodegenerative disorders and life-span extension (Sudarsanam and Johnson, 2010). mTOR is frequently hyperactivated in cancer (Inoki *et al*., 2003; Shor *et al*., 2009), and is thus a clinical target of drug development (Shor *et al*., 2009). mTOR is controlled by cellular energy status via the energy sensor, AMP-activated protein kinase (AMPK) (Inoki *et al*., 2003). A decrease in intracellular ATP is associated with elevated AMP levels, which, in concert with the upstream kinase LKB1, stimulate full activation of AMPK (Hawley *et al*., 1996; Stein *et al*., 2000; Hardie and Hawley, 2001; Shaw *et al*., 2005). Next, AMPK coordinates cellular events to restore the energy balance by promoting cellular ATP production and reducing ATP consumption via shutdown of mTOR-dependent protein translation, a major consumer of cellular energy (Inoki *et al*., 2003; Towler and Hardie, 2007). Low-glucose conditions, or treatment with the synthetic glucose analog 2-deoxyglucose (2-DG), depletes the energy of cancer cells and concurrently induces a fall in mTOR activity, mediated via LKB1/AMPK, an energy stress-sensing signaling pathway (Dennis *et al*., 2001). However, the molecular mechanisms underlying mTOR suppression under conditions of energy stress are yet to be clearly defined. Recent studies have shown that Redd1 has a key role in signal integration, depending on the activation status of LKB/AMPK, to promote inhibition of mTOR activity in a TSC-dependent manner during energy stress (Sofer *et al*., 2005; Schneider *et al*., 2008).

Redd1 was initially identified as a gene induced by hypoxia and DNA damage via the actions of hypoxia-inducible factor 1 and p53/p63 (Ellisen *et al*., 2002; Brugarolas *et al*., 2004). Hypoxia or energy stress promotes binding of Redd1 to the 14-3-3 protein, releasing TSC2 to suppress mTOR activity (DeYoung *et al*., 2008). In addition, Redd1 is required to inhibit mTOR activity under other conditions of cellular stress, including endoplasmic reticulation (ER) and oxidative

Correspondence: Dr H-O Jin or Dr I-C Park, Division of Radiation Cancer Research, Korea Institute of Radiological & Medical Sciences, 215-4 Gongneung-dong, Nowon-gu, Seoul 139-706, Republic of Korea.
E-mail: hyeonok@kirams.re.kr or parkic@kirams.re.kr
Received 16 August 2010; revised 15 February 2011; accepted 17 February 2011; published online 4 April 2011

stress (Whitney *et al*., 2009; Jin *et al*., 2009b), and glucocorticoid treatment (Wang *et al*., 2006a).

TXNIP (also known as VDUP1 or TBP2) interacts with thioredoxin (TRX) and negatively modulates TRX expression and TRX antioxidant function during redox regulation (Fidler and Radinsky, 1996; Chung *et al*., 2006; Nakamura *et al*., 2006). TXNIP is induced by various types of cellular stress, including oxidative stress, UV irradiation, heat shock and apoptotic signaling (Fidler and Radinsky, 1996), and is often suppressed in various human tumors (Goldberg *et al*., 2003; Nakamura *et al*., 2006). Overexpression of TXNIP inhibits proliferation via cell-cycle arrest and promotes apoptosis (Sheth *et al*., 2006). We here demonstrate that TXNIP interacts specifically with Redd1 using a yeast two-hybrid screen.

In the present study, we show that both Redd1 and TXNIP are induced by 2-DG. Redd1 expression is dominantly regulated by activating transcription factor 4 (ATF4) in response to 2-DG. TXNIP stabilizes Redd1 by binding to the protein, resulting in inhibition of mTOR activity. These findings support a novel role for TXNIP, a newly identified member of the mTOR upstream signaling pathway, as a negative regulator in response to stress signals.

Results

2-DG stimulates Redd1 expression and inhibits mTOR activity in a LKB1/AMPK-dependent or -independent manner

In view of the earlier finding that 2-DG activates AMPK/Redd1 signaling leading to inhibition of mTOR activity in head-and-neck squamous cell carcinoma (Schneider *et al*., 2008), we initially determined whether AMPK activity was required for Redd1 expression and consequent suppression of mTOR activity in response to 2-DG. 2-DG-induced Redd1 expression was evaluated in various cancer cell lines with or without LKB1, and phosphorylation of AMPK at Thr172 was assessed to evaluate the functional status of LKB1. As expected, 2-DG stimulated phosphorylation of AMPK in H1299 cells containing wild-type LKB1, but not in HeLa or H460 cells expressing mutant LKB1 (Figure 1a). In contrast, Redd1 was induced by 2-DG in all cell lines, even in the absence of AMPK activation (Figures 1a and b), suggesting that 2-DG stimulates Redd1 expression via a mechanism independent of LKB1/AMPK signaling. Furthermore, 2-DG treatment led to suppression of mTOR activity, estimated by measuring the decrease in S6 phosphorylation, in all cancer cell lines (Figure 1a).

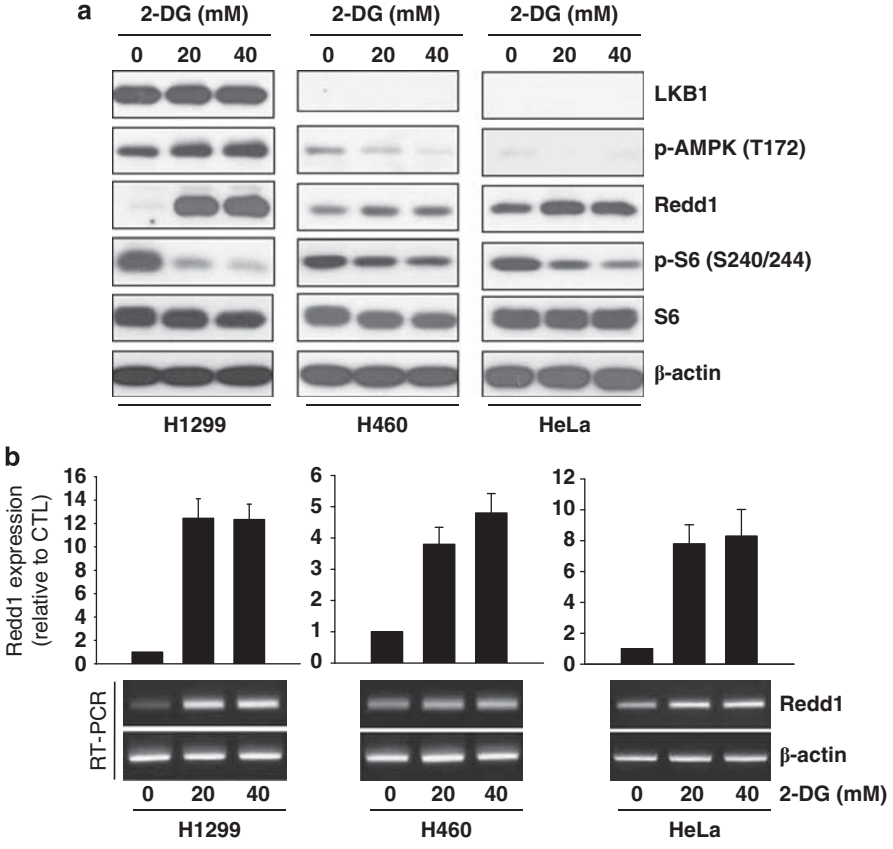

Figure 1 2-DG induces Redd1 expression in a LKB1/AMPK-independent manner. H1299, H460 and HeLa cells were treated with the indicated concentrations of 2-DG for 6 h. The indicated protein levels were measured using western blot analysis (**a**). The indicated mRNA levels were measured with real-time PCR (upper panel) and RT–PCR (low panel) (**b**). Experiments were performed in triplicate.

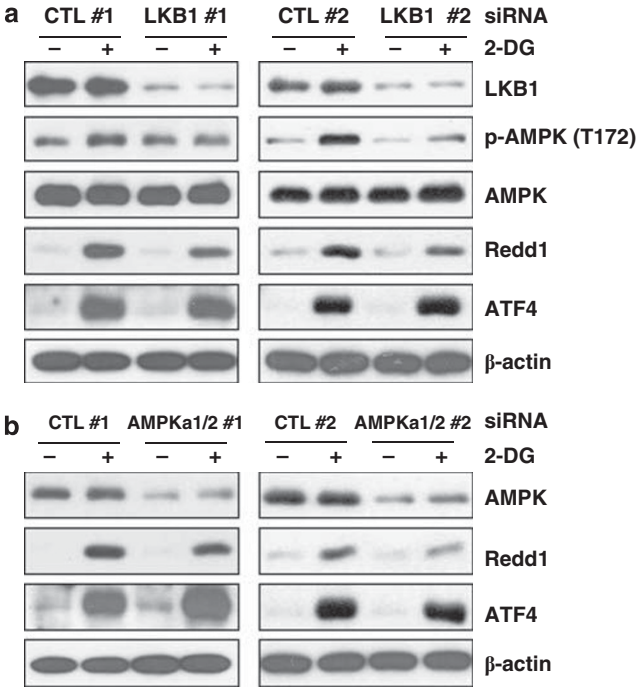

Figure 2 2-DG-induced Redd1 expression is dependent on LKB1/AMPK. H1299 cells were transfected with siCTL or siLKB1 (**a**) or siCTL or siAMPK (**b**) for 20 h, followed by 30 mM 2-DG for 6 h. Protein levels were measured using western blot analysis.

Next, we investigated whether 2-DG-induced Redd1 expression required LKB1/AMPK signaling. LKB1 and AMPK small interfering RNAs (siRNAs) were transiently transfected into the wild-type LKB1-containing cell line, H1299. Downregulation of LKB1/AMPK signaling activation led to a slight decrease in Redd1 expression induced by 2-DG, indicating regulation of this process by LKB1/AMPK (Figure 2). Our results suggest that 2-DG induces Redd1 expression and inhibits mTOR activity via mechanisms that are both dependent and independent of LKB1/AMPK signaling.

ATF4 is responsible for upregulation of Redd1 expression in response to 2-DG

The results discussed above (Figure 1) supported the possibility that 2-DG induced Redd1 expression independently of the LKB1/AMPK signaling pathway. In view of our previous finding that Redd1 is regulated by ATF4 in response to ER stress (Whitney *et al*., 2009; Jin *et al*., 2009b), and as other studies have found that 2-DG induces ER stress (Little *et al*., 1994; Kang and Hwang, 2006), we further investigated whether 2-DG triggered Redd1 expression via ATF4 activation. ATF4 protein expression and an upstream protein thereof, eIF2α phosphorylation were induced by 2-DG in a dose- and time-dependent manner in all tested cell lines (Figures 3a and c). To evaluate the transcriptional activity of ATF4, we examined the expression patterns of ATF4 downstream genes, including VEGF, CHOP and hTRB3, via reverse transcription (RT)–PCR analysis, in H460 and HeLa cells during 2-DG treatment. Such treatment led to enhanced levels of VEGF, CHOP and hTRB3 mRNAs (Figure 3b). Next, we explored whether ATF4 was responsible for upregulation of Redd1 expression in response to 2-DG. Western blotting analysis disclosed that ATF4 siRNA almost completely blocked upregulation of Redd1 in the presence of 2-DG in H1299, H460 and HeLa cells (Figure 4). Our results thus suggest that Redd1 is predominantly regulated by ATF4 activation in response to 2-DG.

Redd1 protein interacts with TXNIP

We found that TXNIP interacted strongly with Redd1 in a yeast two-hybrid screen (data not shown). To further explore the interactions between Redd1 and TXNIP, we initially performed an *in vitro* binding assay. [^{35}S]-labeled His_6-TXNIP protein was prepared by *in vitro* translation, and glutathione *S*-transferase (GST)–Redd1 protein was purified from recombinant *Escherichia coli*. GST–Redd1 protein interacted with [^{35}S]-labeled His_6-TXNIP *in vitro*, as shown using the GST pulldown assay (Figure 5a). We then analyzed whether Redd1 interacts with TXNIP *in vivo*. We performed immunoprecipitation assays using green fluorescent protein (GFP)- and haemagglutinin (HA)-tagged expression vectors. HA-Redd1 bound efficiently to GFP-TXNIP in both 293T and H1299 cells, as shown in Figures 5b and c. Next, we examined whether endogenous Redd1/TXNIP protein interaction is promoted by 2-DG. As shown in Figures 5d, 2-DG enhanced the endogenous interactions of these two proteins. To further clarify the relationship between Redd1 and TXNIP, localization of the two proteins was assessed following co-transfection of plasmids GFP-Redd1 (Green) and HA-TXNIP (Red) into H460 cells. Both proteins were in the same compartments (Figure 5e), supporting interactions between Redd1 and TXNIP within cells.

TXNIP expression is induced in response to 2-DG

Next, we investigated TXNIP expression in the presence of 2-DG. As shown in Figure 6, 2-DG promoted TXNIP protein and mRNA expression in both H460 and HeLa cells, as observed by western blotting and RT–PCR analyses, respectively. However, we could not detect TXNIP mRNA or protein in H1299 cells despite 2-DG treatment. The data indicate that 2-DG promotes TXNIP expression at the transcriptional level.

TXNIP potentiates Redd1-induced mTOR suppression via stabilization of Redd1 protein

We observed a slight increase in Redd1 expression level at baseline in H460 and HeLa cells containing detectable amounts of TXNIP mRNA and protein. However, Redd1 expression was low in H1299 cells, consistent with the absence of TXNIP (Figures 1 and 6). We thus hypothesized that TXNIP expression was correlated with that of Redd1. Accordingly, we investigated the involvement of TXNIP in Redd1 expression and

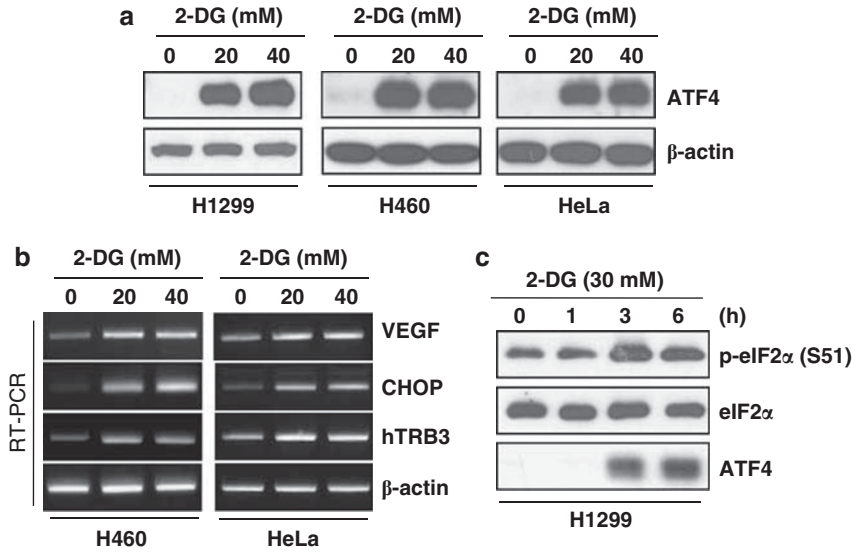

Figure 3 2-DG induces ATF4 transcriptional activity. (**a**, **b**) H1299, H460 and HeLa cells were treated with the indicated concentrations of 2-DG for 6 h. (**c**) H1299 cells were treated with 30 mM 2-DG for the indicated times. Protein levels were measured using western blot analysis (**a**, **c**) and mRNA levels with RT–PCR (**b**). Experiments were performed in duplicate.

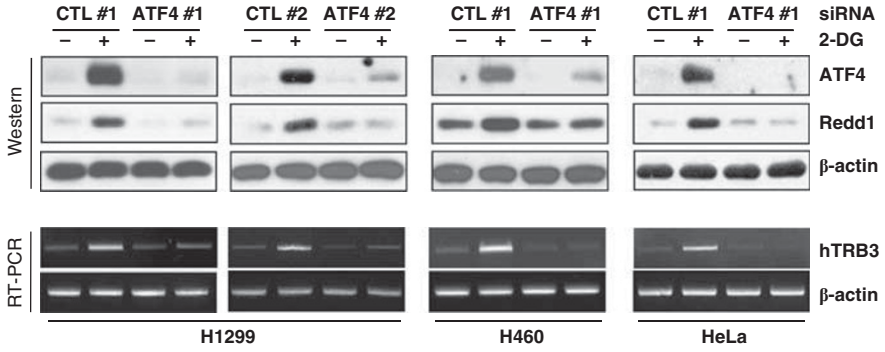

Figure 4 Activated ATF4 stimulates Redd1 expression in response to 2-DG. H1299, H460 and HeLa cells were transfected with siCTL or siATF4 for 20 h, followed by 30 mM 2-DG for 6 h. Protein and mRNA levels were measured via western blot and RT–PCR analyses.

consequent mTOR inhibition. Knockdown of TXNIP expression using specific siRNA blocked upregulation of Redd1 protein and attenuated mTOR activity in HeLa cells growing in the presence of 2-DG, as shown in Figure 7a. Next, HeLa and H1299 cells were transfected with HA-TXNIP plasmids and GFP-Redd1 and different concentrations of HA-TXNIP plasmids, respectively. Overexpression of TXNIP was associated with increased endogenous Redd1 protein expression and a fall in S6 phosphorylation in HeLa cells (Figure 7b). Similar results were obtained with H1299 cells. Specifically, TXNIP overexpression led to an increase in endogenous and exogenous Redd1 protein expression, and decreased S6 phosphorylation (Figure 7c). To test the possibility that TXNIP promoted ATF4 expression, we examined ATF4 protein levels by western blotting. However, ATF4 protein levels were identical in the presence and absence of TXNIP, as shown in Figures 7a and b.

Next, we investigated whether TXNIP promoted Redd1 transcription. RT–PCR revealed that Redd1 mRNA levels were similar in the presence and absence of TXNIP, implying that Redd1 upregulation by TXNIP does not occur at the transcriptional level (Figure 8).

Recent studies have found that Redd1 is degraded through the ubiquitin–proteasome pathway (Katiyar *et al*., 2009). Accordingly, we explored whether TXNIP regulated Redd1 protein stability. We transiently expressed Flag-TXNIP plasmids in H1299 cells and TXNIP siRNAs in HeLa cells, followed by 2-DG treatment and then, upon 2-DG removal, the cells were incubated for different times with cycloheximide treatment to inhibit protein synthesis. As shown in Figures 9a and b, overexpression of TXNIP resulted in significant retardation of Redd1 protein degradation compared with empty vector in the absence or presence of 2-DG (Figure 9a). In contrast, knockdown of TXNIP led to a rapid decrease in the Redd1 protein level compared with control siRNAs (Figure 9b). On the basis of these results, Redd1 protein stability might be

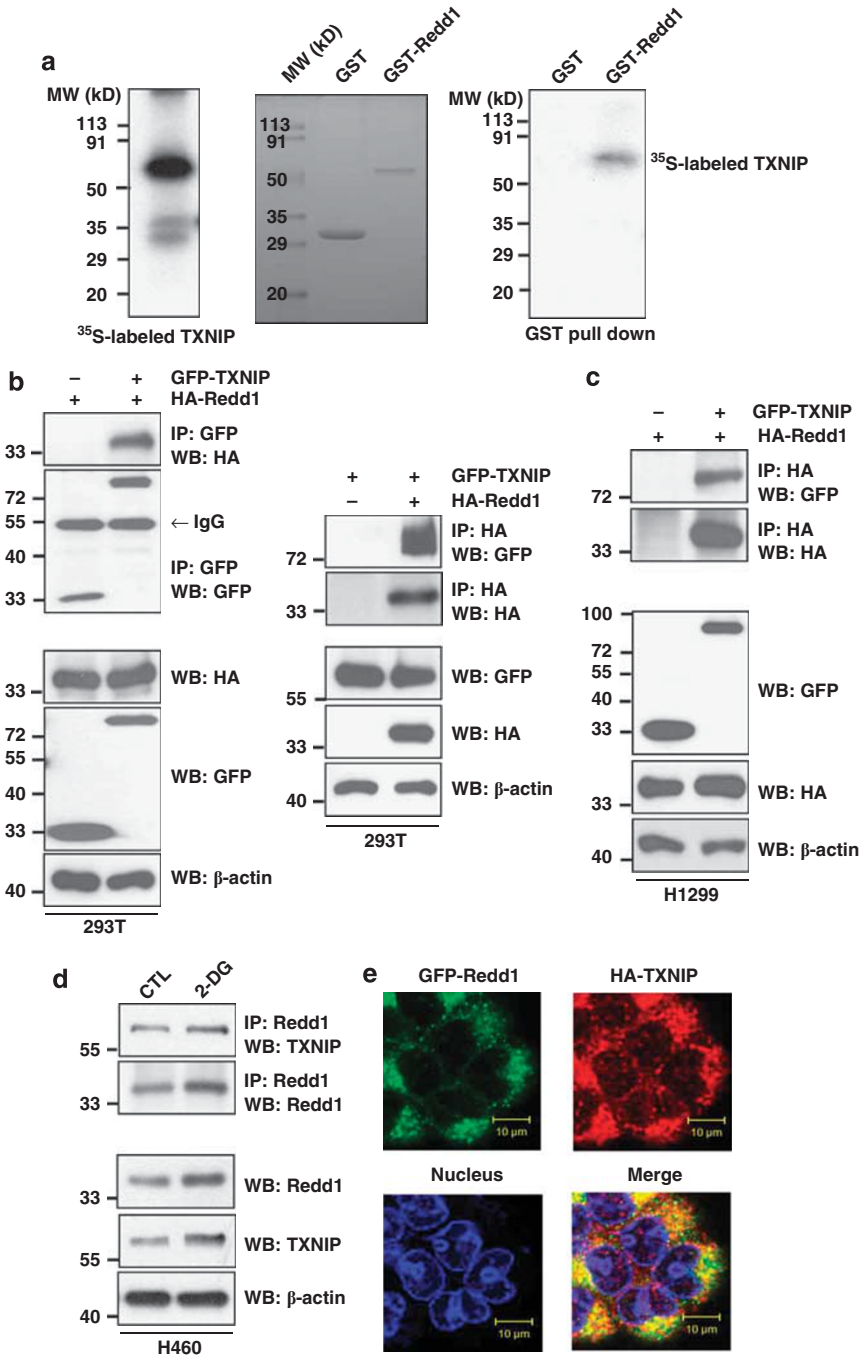

Figure 5 Redd1 interacts with TXNIP. (**a**) *In vitro*-translated TXNIP protein was prepared using a TNT-coupled rabbit reticulocyte translation system and ^{35}S-methionine. GST and GST-Redd1 proteins were overexpressed in BL21 cells and prepared as described in materials and methods. GST-Redd1 proteins bound to glutathione agarose were employed for an *in vitro* binding assay with the ^{35}S-labeled TXNIP protein obtained via *in vitro* translation. The GST-pulldown assay was performed as described in materials and methods. The 10% input and bound proteins were separated by SDS–PAGE and subjected to autoradiography. (**b**, **c**) 293T and H1299 cells were transfected with the indicated plasmids for 24 h. (**d**) H460 cells were treated with 20 mM 2-DG for 6 h. Cell lysates were incubated with protein A/G plus agarose conjugated with the specified antibodies. Immunoprecipitates and cell lysates were subjected to western blot analysis. (**e**) GFP-Redd1 and HA-TXNIP plasmids were transfected into H460 cells. After 24 h, cells were stained with anti-HA. The green and red channels were independently applied or overlaid.

promoted by TXNIP. Next, H1299 cells were transfected with GFP-Redd1, Flag-TXNIP or both, followed by treatment with the proteasome inhibitor, MG132. Exogenous Redd1 protein levels were examined to exclude the possibility that MG132 induced Redd1 expression via ATF4 (Jin *et al*., 2009a). As shown in Figure 9c, MG132 treatment increased both exogenous (GFP-Redd1) and endogenous Redd1 protein levels. In H1299 cells, co-treatment with TXNIP and MG132 resulted in a more significant increase in Redd1 protein

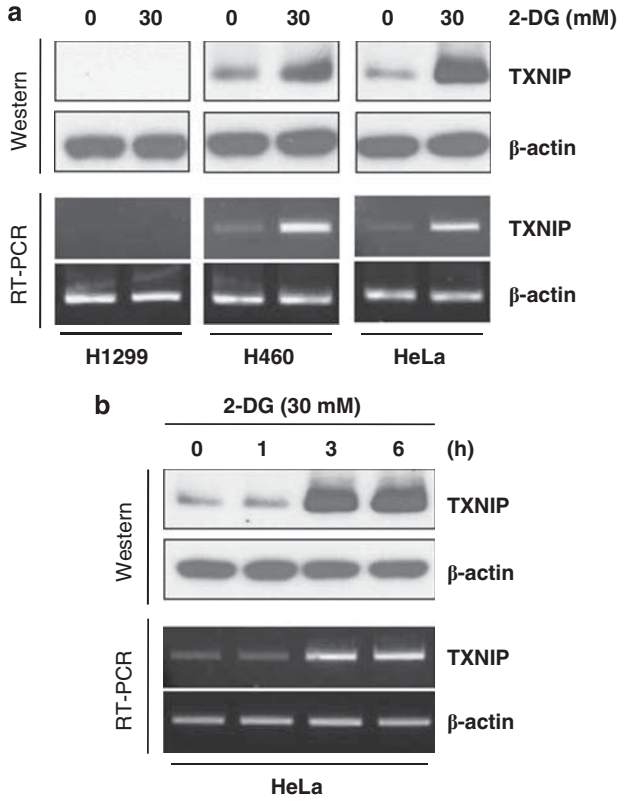

Figure 6 2-DG induces TXNIP expression. (**a**) H1299, H460 and HeLa cells were treated with the indicated concentrations of 2-DG for 6 h. (**b**) H1299 cells were treated with 30 mM 2-DG for the indicated times. TXNIP protein and mRNA levels were measured via western blot and RT–PCR analyses (**a**, **b**). A representative of three independent experiments is shown.

level than was seen when MG132 was used alone. The data collectively indicate that stabilization of Redd1 protein by TXNIP is sufficient to inhibit mTOR activity.

Redd1-induced mTOR inhibition is mediated via binding of TXNIP

To further investigate the importance of TXNIP interactions with Redd1 in mTOR inhibition, we generated N-terminal- (TXNIP-ΔN) and C-terminal-truncated proteins (TXNIP-ΔC), and examined the binding of these proteins to Redd1 *in vitro*. As shown in Figure 10a, GST–Redd1 interacted with [^{35}S]-labeled His_6-TXNIP-ΔN protein. To determine whether N-terminal-truncated TXNIP (TXNIP-ΔN) interacted with Redd1 *in vivo* and whether TXNIP-ΔN was indeed capable of inducing Redd1 protein stability, 293T cells were co-transfected with HA-Redd1 and GFP-TXNIP-ΔC or GFP-TXNIP-ΔN and an immunoprecipitation assay was performed using an anti-HA antibody. As shown in Figure 10b, Redd1 interacted with N-terminal-truncated TXNIP in 293T cells. Overexpression of TXNIP-ΔN led to an increase in Redd1 protein level in cell lysates and Redd1 immunoprecipitates, and a fall in S6 phosphorylation level. The results suggest that Redd1 protein interacts with the C-terminus of TXNIP to increase protein stability, leading to negative regulation of mTOR activity.

Discussion

In the present study, we investigated the mechanism by which Redd1-induced inhibition of mTOR activity is regulated by 2-DG. We report the following: (1) 2-DG induces Redd1 and TXNIP expression; (2) 2-DG-induced Redd1 expression is regulated by ATF4; (3) TXNIP interacts with Redd1 in the cytoplasm; and (4) TXNIP negatively regulates mTOR activity through stabilization of Redd1 protein. To the best of our knowledge, this is the first report of the involvement of TXNIP in Redd1-induced inhibition of mTOR activity in response to 2-DG.

mTOR is a central regulator of protein synthesis, and the activity thereof is modulated by growth factors and nutritional status (Schmelzle and Hall, 2000; Sudarsanam and Johnson, 2010). Dysregulation of mTOR signaling is implicated in cancer (Inoki *et al*., 2003; Shor *et al*., 2009). To date, considerable effort has been focused on elucidating the mechanisms of mTOR signaling, which have emerged as important targets in anti-cancer therapy (Shor *et al*., 2009). A number of proteins, including FKBP38, PRAS40, DEPTOR and Redd1, are involved in regulation of mTOR activity (Sofer *et al*., 2005; Vander Haar *et al*., 2007; Peterson *et al*., 2009). Recently, the stress response gene, Redd1, has been identified as an essential regulator of mTOR activity mediated through the TSC1/2 complex (Sofer *et al*., 2005; DeYoung *et al*., 2008; Schneider *et al*., 2008). Redd1 has a key role in integration of signals, depending on activation of LKB1/AMPK, to promote inhibition of mTOR activity in a TSC-dependent manner (Sofer *et al*., 2005; Schneider *et al*., 2008). Consistent with previous findings, we show that 2-DG inhibits mTOR activity by promoting Redd1 expression via AMPK activation in wild-type LKB1 H1299 cells. However, 2-DG can induce Redd1 expression even in the absence of AMPK activity in the LKB1 mutant cancer cells H460 and HeLa. On the basis of these findings, we propose another possible manner by which 2-DG promotes Redd1 expression. Several reports have shown that 2-DG induces energy depletion and ER stress (Little *et al*., 1994; Kang and Hwang, 2006). Recently, we showed that ER stressor-induced Redd1 expression is regulated by ATF4 (Whitney *et al*., 2009; Jin *et al*., 2009b). In our above experiments, 2-DG triggered Redd1 expression via ATF4 activation. These findings suggest that 2-DG-stimulated Redd1 expression occurs via both LKB1/AMPK-dependent and -independent signaling mechanisms, and is regulated through ATF4 activation.

TXNIP inhibits the antioxidative function of TRX by binding to it (Fidler and Radinsky, 1996; Chung *et al*., 2006; Nakamura *et al*., 2006). Additionally, TXNIP is an important tumor suppressor that inhibits cell proliferation and promotes apoptosis (Sheth *et al*., 2006). In our above experiments, 2-DG stimulated TXNIP mRNA and protein expression in both HeLa and H460 cells. However, in contrast to Redd1, TXNIP expression was not regulated by ATF4 (data not shown). A number of transcriptional factors, including

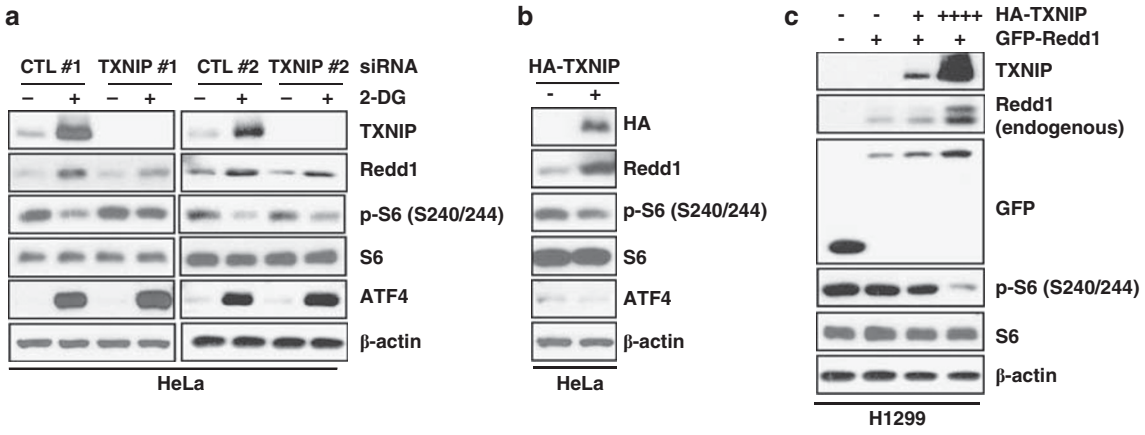

Figure 7 TXNIP induces Redd1 protein expression and inhibits mTOR activity. (**a**) HeLa cells were transfected with siCTL or siTXNIP for 20 h, followed by treatment with 30 mM 2-DG for 6 h. (**b**) HeLa cells were transfected with HA-TXNIP for 30 h. (**c**) H1299 cells were transfected with increasing concentrations of HA-TXNIP, along with GFP-Redd1 for 30 h. Protein levels were measured using western blot analysis.

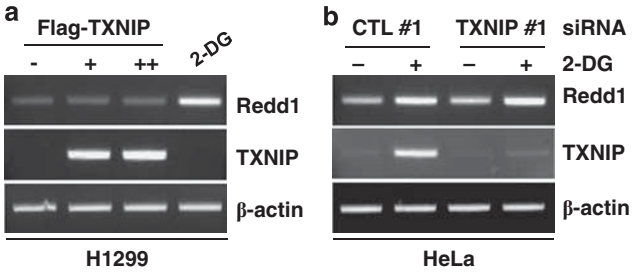

Figure 8 TXNIP does not promote Redd1 mRNA expression. (**a**) H1299 cells were transfected with increasing concentrations of Flag-TXNIP for 24 h. As a control, H1299 cells were treated with 30 mM 2-DG for 4 h. (**b**) HeLa cells were transfected with siCTL or siTXNIP for 20 h, followed by treatment with 30 mM 2-DG for 4 h. The indicated mRNA levels were measured using RT–PCR analysis.

heat shock factor, glucocorticoid receptor, Mondo A and FOXO1, control TXNIP expression under different conditions (Kim *et al*., 2004; Wang *et al*., 2006b; Stoltzman *et al*., 2008). Further studies are required to elucidate the mechanism of TXNIP transcription in the presence of 2-DG.

A yeast two-hybrid screen using Redd1 as bait led to the identification of TXNIP as a binding partner (data not shown). Clearly, Redd1 interacts with TXNIP, both *in vitro* and *in vivo*. Redd1 has been reported to be colocalized with TSC1/2 within membranes in keeping with the rapid and potent effect of Redd1 for mTOR regulation (DeYoung *et al*., 2008). However, a significant portion (>10%) of endogenous Redd1 is localized to the mitochondria, which regulates reactive oxygen species (ROS) (Horak *et al*., 2010). TXNIP is present in both the cytoplasm (Junn *et al*., 2000; Schulze *et al*., 2002, 2004) and nucleus (Nishinaka *et al*., 2004; Saxena *et al*., 2010). TXNIP has also been reported to be present in mitochondria and has been shown to bind the mitochondrially localized TRX (Oka *et al*., 2006). TXNIP localization varies depending on specific cell conditions and cell types (Han *et al*., 2003; Saxena *et al*., 2010).

TXNIP mRNA and protein were detected in H460 and HeLa cells, but not H1299 cells. We observed a slight increase in Redd1 expression at baseline in H460 and HeLa cells that had detectable levels of TXNIP mRNA and protein. However, Redd1 was expressed at a low level in H1299 cells and TXNIP was not present. Accordingly, we postulate that the expression patterns of Redd1 and TXNIP are correlated. Redd1 overexpression did not affect TXNIP mRNA or protein levels. However, TXNIP overexpression was found to promote Redd1 protein expression, concomitant with more reduced mTOR activity in H1299 cells. Knockdown of TXNIP expression using specific siRNA blocked upregulation of Redd1 protein and attenuated mTOR activity in HeLa cells growing in the presence of 2-DG. Our observations support a model whereby the protein stability of Redd1 protein is increased in the presence of TXNIP, leading to increase in Redd1 protein expression in cells, and a consequent increment of mTOR inhibition. Therefore, TXNIP might be needed for an efficient suppression of mTOR in response to metabolic stress. Redd1 additionally bound to the N-terminal-truncated form of TXNIP, which was capable of stabilizing Redd1 protein, leading to inhibition of mTOR activity.

In conclusion, Redd1-induced mTOR inhibition is mediated by ATF4 in response to 2-DG, and TXNIP binds to Redd1 and blocks protein degradation. Our study provides preliminary evidence that TXNIP enhances the stability of Redd1 protein, resulting in inhibition of mTOR activity in response to 2-DG.

Materials and methods

Cell cultures and reagents

HeLa, H1299, H460 and 293T cell lines were obtained from the American Type Culture Collection (Manassas, VA, USA) and cultured in the recommended growth medium (Invitrogen, Carlsbad, CA, USA) under 5% CO_2 at 37 °C. 2-DG was purchased from Sigma–Aldrich (St Louis, MO, USA).

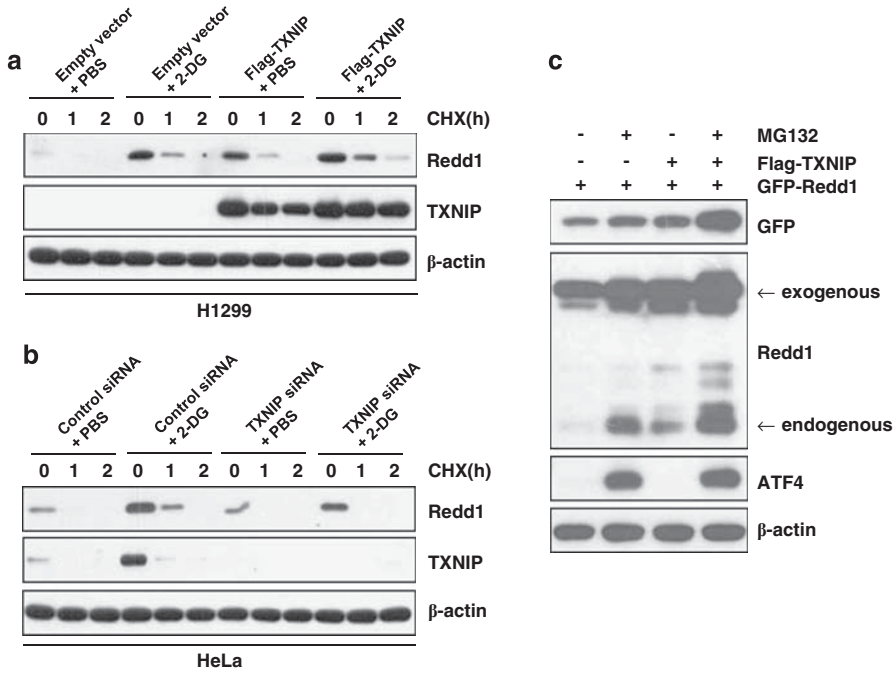

Figure 9 TXNIP regulates the stability of Redd1 protein. (**a**) H1299 cells were transfected with Flag-TXNIP for 24 h and treated with 20 mM 2-DG for 5 h. Media was changed and 30 μg/ml cycloheximide (CHX) was added for the indicated times. (**b**) HeLa cells were transfected with siCTL or siTXNIP for 24 h and treated with 20 mM 2-DG for 5 h. Media were changed and 20 μg/ml CHX was added for the indicated times. (**c**) H1299 cells were transfected with the indicated plasmids and treated with 7 μM MG132 for 5 h. Protein levels were measured using western blot analysis.

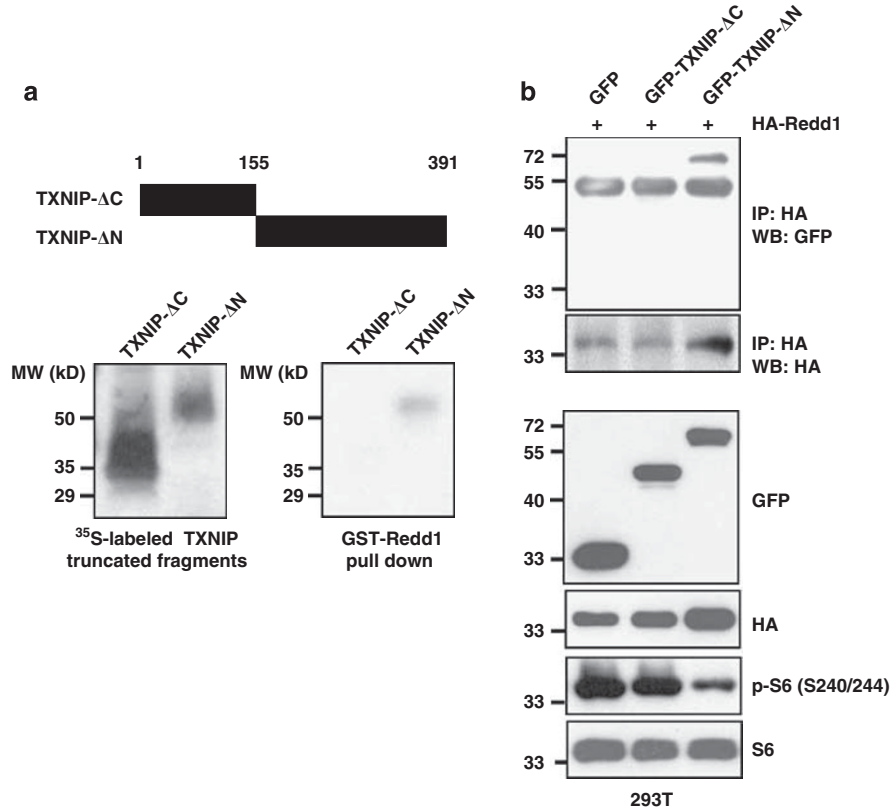

Figure 10 Redd1-induced mTOR inhibition is mediated via interactions with TXNIP. (**a**) GST-Redd1 proteins bound to glutathione agarose were used for an *in vitro* binding assay with ^{35}S-labeled TXNIP-truncated proteins obtained by *in vitro* translation. The GST-pulldown assay was performed as described in materials and Methods. The 10% input and bound proteins were separated by SDS–PAGE analysis and subjected to autoradiography. (**b**) 293T cells were transfected with the indicated plasmids for 30 h. Immunoprecipitates and cell lysates were subjected to western blot analysis.

Isolation of RNA and RT–PCR analysis
Total RNA was isolated from cells using the Easy BLUETM Total RNA extraction kit, according to the manufacturer's directions (iNtRON Biotechnology, Seoul, Republic of Korea). cDNA primed with oligo dT was prepared from 2 μg of total RNA using M-MLV reverse transcriptase (Invitrogen). The following specific primers were used for PCR: Redd1 (5′-AGCCAGTTGGTAAGCCAGG-3′ and 5′-GCCAGAGT CGTGAGTCCAG-3′, 199 bp product), TXNIP (5′-CCTCTG GGAACATCCTCCAA-3′ and 5′-ATTGGCAAGGTAAGT GTGGC-3′, 349 bp product), VEGF (5′-GCATTGGAGCC TTGCCTTGC-3′ and 5′-GCTCATCCTCCTATGTGC-3′, 340 bp product), CHOP (5′-CAGACTGATCCAACTGCAG-3′ and 5′-GACTGGAATCTGGAGAGTG-3′, 280 bp product), hTRB3 (5′-GCCACTGCCTCCCGTCTTG-3′ and 5′-GCTGCC TTGCCCGAGTATGA-3′, 539 bp product) and β-actin (5′-GG ATTCCTATGTGGGCGACGA-3′ and 5′-CGCTCGGTGAGG ATCTTCATG-3′, 438 bp product).

Real-time PCR
Real-time PCR was conducted as described previously (Jin *et al*., 2009a). Primer sequences for real-time PCR were as follows: Redd1 (5′-GAACTCCCACCCCAGATCGG-3′ and 5′-CCACTGTTGCTGCTGTCCAG-3′, 123 bp product) and β-actin (5′-GGATTCCTATGTGGGCGACGA-3′ and 5′-GA GTCCATCACGATGCCAGTG-3′, 315 bp product). Data were expressed as means ± s.d. of three independent experiments for fold induction, relative to the control groups.

Immunoprecipitation experiments
293T and H1299 cell lines were transfected with various combinations of expression vectors. Cells were washed with ice-cold phosphate-buffered saline (PBS) and lysed in lysis buffer (0.5% NP40, 2 mM EDTA, 20 mM Tris-HCl, pH 8.0, 100 mM NaCl, 50 mM β-glycerophosphate, 10 mM NaF) supplemented with a protease inhibitor cocktail (Roche, Mannheim, Germany). Cell lysates were precleared with protein A/G plus agarose (Santa Cruz Biotechnology, Santa Cruz, CA, USA), and incubated with antibody and protein A/G plus agarose overnight at 4 °C. Pellets were washed four times with lysis buffer, resuspended in sample buffer, and analyzed using SDS-polyacrylamide gel electrophoresis (SDS–PAGE).

Plasmids and siRNAs
Full-length Redd1 cDNA was cloned into the EcoRI sites of pcDNA-HA (Invitrogen) encoding HA, EcoRI/BamHI sites of pEGFP-C1 (Clontech, Mountain View, CA, USA) encoding GFP for expression in mammalian cells, and BamHI/EcoRI sites of pGEX-6P-3 (Amersham Pharmacia Biotech, Uppsala, Sweden) encoding GST for expression in *E. coli*. Constructs of full-length TXNIP cDNA in mammalian pEGFP-C1 (BD Bioscience Clontech, San Diego, CA, USA) and *E. coli* pRSET-C (Invitrogen) were kindly provided by Dr Junji Yodoi (Kyoto University, Kyoto, Japan). Full-length and truncated TXNIP (TXNIP-ΔC; 1–154 aa and TXNIP-ΔN; 155–391 aa) incorporating EcoRI sites at the ends were generated by PCR and cloned into the corresponding sites of pCMV Tag 2B encoding Flag, pcDNA-HA and pEGFP-C2. All constructs were verified by DNA sequencing.

TXNIP (#1, SC-44943; #2, J-010814-05-0005), ATF4 (#1, sc-35112; #2, J-005125-10-0005), LKB1 (#1, sc-35816; #2, J-005035-07-0005), AMPKα1/2 (#1, sc-45312; #2, J-005027-06-0005 and J-005361-06-0005) and control siRNAs (#1, sc-37007; #2, D-001810-01-05) were purchased from Santa Cruz Biotechnology and Thermo Scientific Dharmacon (Chicago, IL, USA). Transfection experiments with plasmids and siRNAs were performed using Lipofectamine Plus and Lipofectamine 2000, respectively, according to the manufacturer's instructions (Invitrogen).

Preparation of recombinant proteins and in vitro *binding assay*
In vitro-translated full-length and truncated TXNIP proteins were prepared using a TNT-coupled rabbit reticulocyte translation system (Promega, Madison, WI, USA) and ^{35}S-Methionine. For preparation of GST and GST–Redd1 proteins, *E. coli* strain BL21 transformed with each expression plasmid was treated with 0.2 mM isopropyl-β-D-thiogalactoside for 3 h. Pelleted cells were lysed in PBS containing 1% Triton X-100 and protease inhibitor cocktail by sonication. After centrifugation, supernatant fractions were applied to glutathione agarose and *in vitro*-translated full-length and truncated TXNIP proteins for 3 h. Beads were washed three times with PBS and resuspended in sample buffer. Bound proteins were subjected to electrophoresis on an 8–18% gradient gel, which was subsequently processed for autoradiography.

Immunofluorescence microscopy
H460 cells were plated onto 12-well plates containing 13 mm non-coated glass coverslips (Fisher Scientific, Pittsburgh, PA, USA) for 24 h. Cells were transfected with HA-TXNIP and GFP-Redd1. The coverslips were incubated with anti-HA antibody, followed by rhodopsin-conjugated anti-mouse secondary antibody (Vector Laboratories, Burlingame, CA, USA). Nuclei were counterstained using DAPI (Invitrogen–Molecular Probes, Eugene, OR, USA). Next, coverslips were mounted with Vectashield mounting medium (Vector Laboratories) and analyzed via confocal microscopy (LSM-510, Carl Zeiss, Oberkochen, Germany).

Western blot analysis
Cell lysates and immunoprecipitates were separated by SDS–PAGE and transferred to nitrocellulose membranes, followed by immunoblotting with the specified primary antibodies and horseradish peroxidase-conjugated secondary antibodies. Immunoreactive bands were visualized with SuperSignal West Pico Chemiluminescent Substrates (Thermo Scientific Pierce, Rockford, IL, USA). The antibody to Redd1 was obtained from the ProteinTech Group (Chicago, IL, USA), antibody to TXNIP from Medical & Biological Laboratories (Nagoya, Japan), antibodies to p-eIF2α (Ser51), p-S6 (Ser240/244) and S6 from Cell Signaling Technology (Beverly, MA, USA), and antibodies to ATF4, eIF2α, His, HA, GFP, and TRX from Santa Cruz Biotechnology. β-Actin was acquired from Sigma–Aldrich.

Conflict of interest

The authors declare no conflict of interest.

Acknowledgements

This work was supported by the National Nuclear R&D Program and the Basic Science Research Program and the National Research Foundation of Korea (NRF) funded by the Ministry of Education, Science and Technology (2010-0009503) in Republic of Korea.

References

Brugarolas J, Lei K, Hurley RL, Manning BD, Reiling JH, Hafen E *et al*. (2004). Regulation of mTOR function in response to hypoxia by REDD1 and the TSC1/TSC2 tumor suppressor complex. *Genes Dev* **18**: 2893–2904.

Chung JW, Jeon JH, Yoon SR, Choi I. (2006). Vitamin D3 upregulated protein 1 (VDUP1) is a regulator for redox signaling and stress-mediated diseases. *J Dermatol* **33**: 662–669.

Dennis PB, Jaeschke A, Saitoh M, Fowler B, Kozma SC, Thomas G. (2001). Mammalian TOR: a homeostatic ATP sensor. *Science* **294**: 1102–1105.

DeYoung MP, Horak P, Sofer A, Sgroi D, Ellisen LW. (2008). Hypoxia regulates TSC1/2-mTOR signaling and tumor suppression through REDD1-mediated 14-3-3 shuttling. *Genes Dev* **22**: 239–251.

Ellisen LW, Ramsayer KD, Johannessen CM, Yang A, Beppu H, Minda K *et al*. (2002). REDD1, a developmentally regulated transcriptional target of p63 and p53, links p63 to regulation of reactive oxygen species. *Mol Cell* **10**: 995–1005.

Fidler IJ, Radinsky R. (1996). Search for genes that suppress cancer metastasis. *J Natl Cancer Inst* **88**: 1700–1703.

Goldberg SF, Miele ME, Hatta N, Takata M, Paquette-Straub C, Freedman LP *et al*. (2003). Melanoma metastasis suppression by chromosome 6: evidence for a pathway regulated by CRSP3 and TXNIP. *Cancer Res* **63**: 432–440.

Han SH, Jeon JH, Ju HR, Jung U, Kim KY, Yoo HS *et al*. (2003). VDUP1 upregulated by TGF-beta1 and 1,25-dihydorxyvitamin D3 inhibits tumor cell growth by blocking cell-cycle progression. *Oncogene* **22**: 4035–4046.

Hardie DG, Hawley SA. (2001). AMP-activated protein kinase: the energy charge hypothesis revisited. *Bioessays* **23**: 1112–1119.

Hawley SA, Davison M, Woods A, Davies SP, Beri RK, Carling D *et al*. (1996). Characterization of the AMP-activated protein kinase from rat liver and identification of threonine 172 as the major site at which it phosphorylates AMP-activated protein kinase. *J Biol Chem* **271**: 27879–27887.

Horak P, Crawford AR, Vadysirisack DD, Nash ZM, DeYoung MP, Sgroi D *et al*. (2010). Negative feedback control of HIF-1 through REDD1-regulated ROS suppresses tumorigenesis. *Proc Natl Acad Sci USA* **107**: 4675–4680.

Inoki K, Zhu T, Guan KL. (2003). TSC2 mediates cellular energy response to control cell growth and survival. *Cell* **115**: 577–590.

Jin HO, Seo SK, Woo SH, Choe TB, Hong SI, Kim JI *et al*. (2009a). Nuclear protein 1 induced by ATF4 in response to various stressors acts as a positive regulator on the transcriptional activation of ATF4. *IUBMB Life* **61**: 1153–1158.

Jin HO, Seo SK, Woo SH, Kim ES, Lee HC, Yoo DH *et al*. (2009b). Activating transcription factor 4 and CCAAT/enhancer-binding protein-beta negatively regulate the mammalian target of rapamycin via Redd1 expression in response to oxidative and endoplasmic reticulum stress. *Free Radic Biol Med* **46**: 1158–1167.

Junn E, Han SH, Im JY, Yang Y, Cho EW, Um HD *et al*. (2000). Vitamin D3 up-regulated protein 1 mediates oxidative stress via suppressing the thioredoxin function. *J Immunol* **164**: 6287–6295.

Kang HT, Hwang ES. (2006). 2-Deoxyglucose: an anticancer and antiviral therapeutic, but not any more a low glucose mimetic. *Life Sci* **78**: 1392–1399.

Katiyar S, Liu E, Knutzen CA, Lang ES, Lombardo CR, Sankar S *et al*. (2009). REDD1, an inhibitor of mTOR signalling, is regulated by the CUL4A-DDB1 ubiquitin ligase. *EMBO Rep* **10**: 866–872.

Kim KY, Shin SM, Kim JK, Paik SG, Yang Y, Choi I. (2004). Heat shock factor regulates VDUP1 gene expression. *Biochem Biophys Res Commun* **315**: 369–375.

Little E, Ramakrishnan M, Roy B, Gazit G, Lee AS. (1994). The glucose-regulated proteins (GRP78 and GRP94): functions, gene regulation, and applications. *Crit Rev Eukaryot Gene Expr* **4**: 1–18.

Nakamura H, Masutani H, Yodoi J. (2006). Extracellular thioredoxin and thioredoxin-binding protein 2 in control of cancer. *Semin Cancer Biol* **16**: 444–451.

Nishinaka Y, Masutani H, Oka S, Matsuo Y, Yamaguchi Y, Nishio K *et al*. (2004). Importin alpha1 (Rch1) mediates nuclear translocation of thioredoxin-binding protein-2/vitamin D(3)-up-regulated protein 1. *J Biol Chem* **279**: 37559–37565.

Oka S, Liu W, Masutani H, Hirata H, Shinkai Y, Yamada S *et al*. (2006). Impaired fatty acid utilization in thioredoxin binding-2 (TBP-2)-deficient mice: a unique animal model of Reye syndrome. *FASEB J* **20**: 121–123.

Peterson TR, Laplante M, Thoreen CC, Sancak Y, Kang SA, Kuehl WM *et al*. (2009). DEPTOR is an mTOR inhibitor frequently overexpressed in multiple myeloma cells and required for their survival. *Cell* **137**: 873–886.

Saxena G, Chen J, Shalev A. (2010). Intracellular shuttling and mitochondrial function of thioredoxin-interacting protein. *J Biol Chem* **285**: 3997–4005.

Schmelzle T, Hall MN. (2000). TOR, a central controller of cell growth. *Cell* **103**: 253–262.

Schneider A, Younis RH, Gutkind JS. (2008). Hypoxia-induced energy stress inhibits the mTOR pathway by activating an AMPK/REDD1 signaling axis in head and neck squamous cell carcinoma. *Neoplasia* **10**: 1295–1302.

Schulze PC, De Keulenaer GW, Yoshioka J, Kassik KA, Lee RT. (2002). Vitamin D3-upregulated protein-1 (VDUP-1) regulates redox-dependent vascular smooth muscle cell proliferation through interaction with thioredoxin. *Circ Res* **91**: 689–695.

Schulze PC, Yoshioka J, Takahashi T, He Z, King GL, Lee RT. (2004). Hyperglycemia promotes oxidative stress through inhibition of thioredoxin function by thioredoxin-interacting protein. *J Biol Chem* **279**: 30369–30374.

Shaw RJ, Lamia KA, Vasquez D, Koo SH, Bardeesy N, Depinho RA *et al*. (2005). The kinase LKB1 mediates glucose homeostasis in liver and therapeutic effects of metformin. *Science* **310**: 1642–1646.

Sheth SS, Bodnar JS, Ghazalpour A, Thipphavong CK, Tsutsumi S, Tward AD *et al*. (2006). Hepatocellular carcinoma in Txnip-deficient mice. *Oncogene* **25**: 3528–3536.

Shor B, Gibbons JJ, Abraham RT, Yu K. (2009). Targeting mTOR globally in cancer: thinking beyond rapamycin. *Cell Cycle* **8**: 3831–3837.

Sofer A, Lei K, Johannessen CM, Ellisen LW. (2005). Regulation of mTOR and cell growth in response to energy stress by REDD1. *Mol Cell Biol* **25**: 5834–5845.

Stein SC, Woods A, Jones NA, Davison MD, Carling D. (2000). The regulation of AMP-activated protein kinase by phosphorylation. *Biochem J* **345**: 437–443.

Stoltzman CA, Peterson CW, Breen KT, Muoio DM, Billin AN, Ayer DE. (2008). Glucose sensing by MondoA:Mlx complexes: a role for hexokinases and direct regulation of thioredoxin-interacting protein expression. *Proc Natl AcadSci USA* **105**: 6912–6917.

Sudarsanam S, Johnson DE. (2010). Functional consequences of mTOR inhibition. *Curr Opin Drug Discov Devel* **13**: 31–40.

Towler MC, Hardie DG. (2007). AMP-activated protein kinase in metabolic control and insulin signaling. *Circ Res* **100**: 328–341.

Vander Haar E, Lee SI, Bandhakavi S, Griffin TJ, Kim DH. (2007). Insulin signalling to mTOR mediated by the Akt/PKB substrate PRAS40. *Nat Cell Biol* **9**: 316–323.

Wang H, Kubica N, Ellisen LW, Jefferson LS, Kimball SR. (2006a). Dexamethasone represses signaling through the mammalian target of rapamycin in muscle cells by enhancing expression of REDD1. *J Biol Chem* **281**: 39128–39134.

Wang Z, Rong YP, Malone MH, Davis MC, Zhong F, Distelhorst CW. (2006b). Thioredoxin-interacting protein (txnip) is a glucocorticoid-regulated primary response gene involved in mediating glucocorticoid-induced apoptosis. *Oncogene* **25**: 1903–1913.

Whitney ML, Jefferson LS, Kimball SR. (2009). ATF4 is necessary and sufficient for ER stress-induced upregulation of REDD1 expression. *Biochem Biophys Res Commun* **379**: 451–455.